Random-barrier and hierarchical relaxation in $K_{1-x}Li_xTaO_3$

1991 J. Phys.: Condens. Matter 3 8387

(http://iopscience.iop.org/0953-8984/3/43/006)

J. Phys.: Condens. Matter 3 (1991) 8387–8401. Printed in the UK

Random-barrier and hierarchical relaxation in $K_{1-x}Li_xTaO_3$

Hans-Martin Christen†, Ulrich T Höchli†, André Châtelain‡ and Saul Ziolkiewicz§

† IBM Research Division, Zurich Research Laboratory, CH-8803 Rüschlikon, Switzerland

‡ Institut de Physique Expérimentale, Swiss Federal Institute of Technology, CH-1015 Lausanne, Switzerland

§ Laboratoire d'Acoustique et Optique de la Matière Condensée, Université Pierre et Marie Curie, Boîte 78, F-75252 Paris Cédex 05, France

Received 28 May 1991

Abstract. Two complete data sets of the dependence of dielectric permittivity on temperature and frequency in the range of 10^{-3} to 10^9 Hz are reported for $K_{1-x}Li_xTaO_3$, $x = 0.025$ and $x = 0.033$, with two impurity-induced relaxation branches observed in detail. It is shown that in the $x = 0.033$ samples, relaxation in the low-frequency branch crosses over from random-barrier to hierarchical behaviour as the temperature is lowered. For the first time we fit the expressions describing each type of relaxation to both depolarization current and dielectric permittivity data, allowing a crossover temperature to be determined. In addition, a detailed study of the high-frequency branch gives new insight into its quite particular behavior. It is also shown that within experimental error, the dielectric properties of the sample do not depend on the method of growth.

1. Introduction

The mixed-crystal system $K_{1-x}Li_xTiO_3$ has been investigated in considerable detail (Höchli, Knorr and Loidl 1990). Its characteristics are dipole moments associated with Li impurities occupying K sites at random and displaced with respect to the centrosymmetric K site by about 1 Å (Van der Klink *et al* 1983). Interaction between these moments leads to a low-temperature ground state devoid of long-range polar order. A combined second-harmonic light generation and birefringence investigation revealed a dipolar correlation length of tens of nanometers (Azzini *et al* 1991), defined as the distance at which the moments change from $+z$ to $-z$. The quadrupolar correlation length, implying changes from $\pm z$ to $\pm x$ or $\pm y$, was however of the order of 500 nm (Azzini *et al* 1991, Prater *et al* 1981). The question of how such a peculiar cluster configuration can form was not addressed.

Studies of the dynamics of $K_{1-x}Li_xTaO_3$ showed that the dielectric relaxation is highly polydispersive and that the shape of the loss curve is temperature dependent (Höchli 1982). At Li concentrations of about 4%, two relaxation branches are present and it has been suggested that they belong to $\pi/2$ and π flips, i.e. jumps by 90° and 180°, of Li dipoles between equivalent [100] displacements (Höchli and Baeriswyl 1984).

0953-8984/91/438387 + 15 $03.50

These branches have been named quadrupolar and dipolar relaxation, where dipolar refers to impurity motion without a change in the electric quadrupolar moment (i.e. π flips), while in quadrupolar relaxation both dipolar and quadrupolar moments change. The distinction between $\pi/2$ and π flips is afforded by measurements of the elastic (or quadrupolar) susceptibility on the same sample (Doussineau *et al* 1991, Höchli *et al* 1991). The important question of whether one is dealing with parallel relaxation (distribution of relaxation times) or series relaxation (hierarchical dynamics) has not yet been answered conclusively. In fact, it is necessary to fit model predictions for each type of relaxation to data over a very large temperature and frequency range, and to compare the quality of the fits at each temperature. This requires detailed knowledge regarding dielectric properties and a certain computational effort. We thus wish to present the two most complete data sets extending from 10^{-3} to 10^{9} Hz and from 30 to 180 K on two samples in which both $\pi/2$ and π relaxation branches are observed. This is the case for $x \simeq 0.03$. Since this concentration range is narrow and observations critically depend on it, we will also report test measurements on control samples grown by different methods. The purpose is to evaluate the results in terms of model expressions proposed quite generally for dielectric relaxation and to relate the parameters describing these expressions to microscopic models of relaxation mechanisms.

2. Mathematical preliminary

In this section we give short definitions of the dielectric properties and of the Debye–Wagner expression. Since it does not contain new results, it can be skipped by the reader familiar with dielectric investigations. We will report on the behavior of the complex dielectric constant, or relative dielectric permittivity, $\varepsilon^* = \varepsilon' - j\varepsilon''$ as a function of the frequency of the applied field. The intensity of the field is kept at sufficiently low values so that linearity can be assumed. Under this condition, the negative time derivative of the normalized decay function $f(t) = -dF/dt$ is given as the one-sided Fourier transform, or purely imaginary Laplace transform, of the normalized dielectric constant $(\Delta\varepsilon)^{-1}(\varepsilon^* - \varepsilon_\infty)$, where $\Delta\varepsilon = \varepsilon(0) - \varepsilon_\infty$ is the relaxation step, and $\varepsilon(0)$ and ε_∞ are the values that ε^* takes at frequencies much smaller and much larger than the characteristic frequency ω_0 of the relaxation phenomena (Jonscher 1983).

If a sample with dimensions surface × thickness = Sd is charged from $t = -\infty$ to $t = 0$ in a constant field E_0, then the depolarization current is given by $i(t) = S\varepsilon_0 E_0(\varepsilon(0) - 1)f(t)$, where $\varepsilon_0 = 8.85\ \mathrm{pFm^{-1}}$. This, together with the above considerations, yields

$$i(t) = \frac{\varepsilon_0 E_0 S}{2\pi} \int_0^\infty (\varepsilon^*(\omega) - \varepsilon_\infty) e^{j\omega t}\, d\omega. \tag{1}$$

This relates $i(t)$ to the imaginary (and reversible) Laplace transform of $\varepsilon^*(\omega) - \varepsilon_\infty$: depolarization current measurements thus give the same information as dielectric constant determination.

The relation between $\varepsilon' - \varepsilon_\infty$ and ε'' is given by the well-known Kramers–Kronig equations. However, only ε' and ε'' are directly accessible experimentally, whereas in general $\varepsilon' - \varepsilon_\infty$ is not, since ε_∞ must be determined by extrapolation. Therefore, ε' data are more difficult to interpret, and we will only present the results for ε''. The loss curve $\varepsilon''(\ln \omega)$ allows the easiest access to qualitative interpretation: it will show a maximum

for each relaxation process, the relaxation step is $\Delta\varepsilon = (2/\pi)\int\varepsilon''(\ln\omega)\,\mathrm{d}\ln\omega$, and a characteristic width at half maximum can be attributed to the curve $\varepsilon''(\ln\omega)$.

The Debye (1912) model of independently relaxing dipoles, all having the same relaxation time τ_0, predicts this width to be 1.144 decades. Wagner (1913) proposed a distribution of relaxation times $g(\tau)$ to account for larger widths found experimentally, by writing the dielectric permittivity of a composed system as superposition of the individual Debye responses. This also leads to non-exponential decay of the polarization $P(t)$, where $P(t)$ is proportional to the decay function $F(t)$, and

$$1 - \int_0^t f(\tau)\,\mathrm{d}\tau = F(t) = \int_0^\infty g(\tau)\mathrm{e}^{-t/\tau}\,\mathrm{d}\tau. \tag{2}$$

The last term of this equation becomes a Laplace transform for $s \equiv 1/\tau$: $F(t) = \int \exp(-st)g(s^{-1})s^{-2}\,\mathrm{d}s$ and, therefore, the inverse Laplace transform of the decay function $F(t)$ gives $\tau^2 g(\tau)$, but numerical calculation of this inverse Laplace transform is an unstable process (Bellmann *et al* 1966).

Given a distribution of relaxation times, one can also quite easily compute the corresponding permittivity $(\Delta\varepsilon)^{-1}(\varepsilon^*(\omega) - \varepsilon_\infty) = \int g(\tau)(1 + \mathrm{j}\omega\tau)^{-1}\,\mathrm{d}\tau$, but once again the inverse is difficult to calculate numerically (Colonomos and Gordon 1979). In terms of these mathematical transforms, however, a distribution $g(\tau)$ can always be associated with a decay current $i(t)$ and identically with a loss curve $\varepsilon''(\ln\omega)$. Wagner (1913) has chosen this distribution to be log-Gaussian, defining what we refer to as the Debye–Wagner permittivity, ε_{DW}. The three parameters to be determine are the relaxation step, $\Delta\varepsilon$, the centre frequency, ω_0 and the width of the Gaussian distribution, Δ. These parameters are obtained by fits minimizing $\chi^2 = \sqrt{[(\varepsilon_{\text{measured}} - \varepsilon_{\text{predicted}})^2]}$ and using a Marquardt algorithm (Press *et al* 1986). If fits of ε_{DW} represent the data reasonably well, then this function can be used to obtain a quantitative description in terms of the fit parameters. This will be done for most of the dielectric spectra presented here.

3. Experiment

3.1. Samples

Four different samples were investigated. Ths first two samples, $K_{0.967}Li_{0.033}TaO_3$ and $K_{0.966}Li_{0.034}TaO_3$ have both been grown by the spontaneous nucleation technique (Van der Klink and Rytz 1982), with the only difference being that an accelerated crucible rotation technique (ACRT) (Elwell and Scheel 1975) was applied for the latter. The second pair of samples, $K_{0.975}Li_{0.025}TaO_3$ and $K_{0.974}Li_{0.026}TaO_3$ were grown by the Czochralski top-seeded solution growth ($K_{0.975}Li_{0.025}TaO_3$) and the ACRT ($K_{0.974}Li_{0.026}TaO_3$) methods. We have chosen such sample pairs in order to allow a comparison between crystals obtained by different growth techniques.

The concentrations of the samples were determined by comparing their dielectric properties to those of standard samples, the concentration of which had been determined by nuclear magnetic resonance (Van der Klink and Rytz, 1982).

The samples were cut from monocrystals with faces along the (100) directions, and gold electrodes were evaporated onto the polished surfaces. Sample size was determined by the following two considerations: first, large sample capacitance yields a better signal–to–noise ratio; second, the sample has to be kept sufficiently small in order to assure compositional homogeneity. Furthermore, Maglione (1987) has shown that resonances

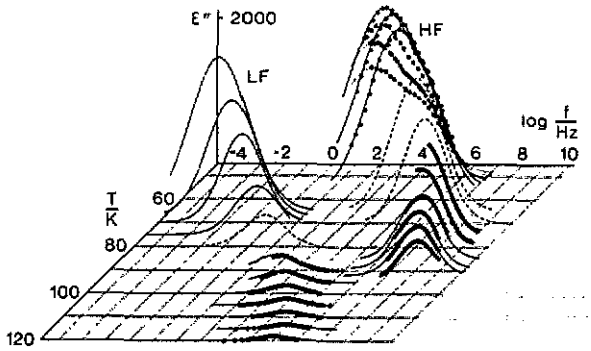

Figure 1. Imaginary part of the dielectric permittivity $\varepsilon''(f, T)$ for $K_{0.967}Li_{0.033}TaO_3$. LF and HF labels stand for low-frequency and high-frequency branches, respectively. The representation of the LF branch also contains curves obtained by using the Gaussian fit-parameters of the DC data in figure 2. Other curves in the LF branch are also fits to a Gaussian distribution, whereas fits for the HF branch are to a double distribution as described in the text. Broken curves are not experimental results but interpolations to guide the eye.

can occur due to standing electromagnetic waves in this material, which has a large refractive index because of the high value of $\varepsilon' \sim 10^3$. To avoid resonances in the accessible frequency range, sample dimensions of the order of 1 mm × 1 mm × 1 mm have been used from 1 MHz to 1 GHz, whereas samples of approximately 1 mm × 3 mm × 3 mm were employed at lower frequencies. In view of the high dielectric constant of the material, stray fields are not a problem even with this apparently unfavourable geometry.

3.2. Apparatus

The dielectric permittivity was measured using conventional bridge (GR1616 and Boonton 75A) and impedance analyzer (hp4191) techniques in the corresponding frequency ranges (10 to 5×10^5 Hz and 10^6 to 10^9 Hz, respectively). Depolarization current (DC) data were taken with a Keithly 642 electrometer after charging the sample in a constant field of 10 kV/m for 5 to 10 times as long as the actual measurement time. Temperature was stabilized to ±0.1 K during the entire experiment. This setup, using a home-manufactured He-flux cryostat, allows measurement times of 3000 s to be achieved routinely. We therefore cover an actual corresponding frequency range of 12 decades from 1 mHz to 1 GHz.

4. Experimental results and evaluation of data

Figure 1 shows a typical $\varepsilon''(\log \omega, T)$ graph for the spontaneous-nucleation grown $K_{0.967}Li_{0.033}TaO_3$ sample. We also show the calculated $\varepsilon''(\log \omega)$ curves that correspond to the parameters obtained by fitting a Gaussian distribution of relaxation times to the

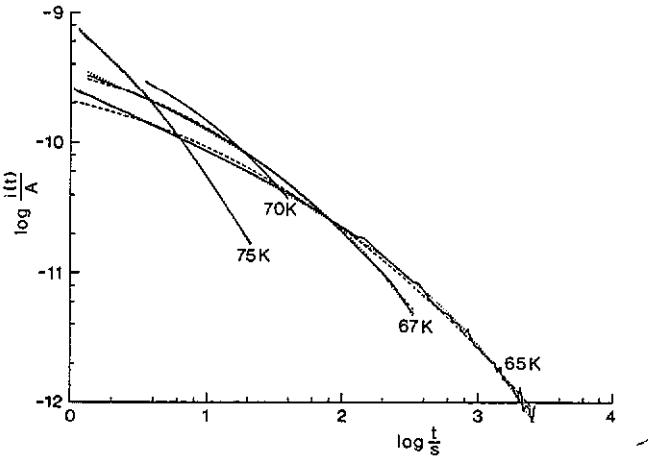

Figure 2. Depolarization current measurements (full curves) for four temperatures and sample $K_{0.967}Li_{0.033}TaO_3$. The parameters of the fits to a Gaussian distribution (broken curve) were used to complete figure 1 at the lowest frequencies. Also shown are fits to the KWW function (dotted curve; largely covered by the full curve) as described in the text.

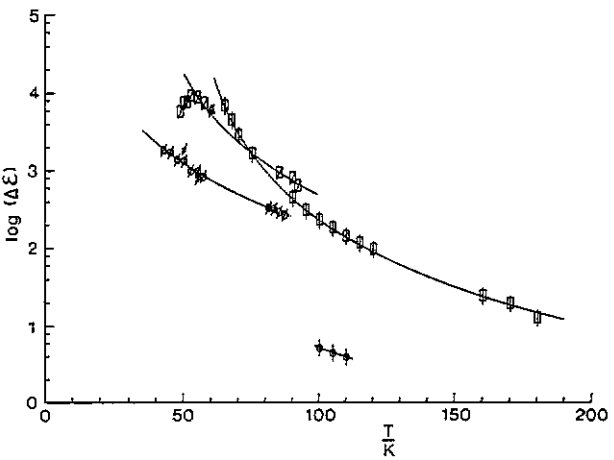

Figure 3. Relaxation step $\Delta\varepsilon$ as obtained from fits to a Gaussian distribution of relaxation times. Results for LF (|) and HF1 (/) (see text) branches of the samples $K_{0.967}Li_{0.033}TaO_3$ (□) and $K_{0.975}Li_{0.025}TaO_3$ (○) are shown. Also shown are isolated data points for the samples $K_{0.966}Li_{0.034}TaO_3$ (△) (at 60 K) and $K_{0.974}Li_{0.026}TaO_3$ (*) (at 50 and 55 K), which allows the samples obtained by different growth methods to be compared. Curves are best fits of $\Delta\varepsilon \propto (T - T_0)^{\gamma}$.

DC data in figure 2. Debye relaxation has also been observed at 45 K and 10^8 Hz (Höchli and Maglione 1989) independently of the concentration and is not shown on figure 1. In this figure, we note two distinct relaxation branches that we call LF and HF for the one appearing at lower and the other at higher frequencies at a given temperature.

The parameters of the Debye–Wagner permittivity for the LF branch are shown in figures 3 to 5. It is seen that the logarithm of the centre frequency is nearly linear in $1/T$

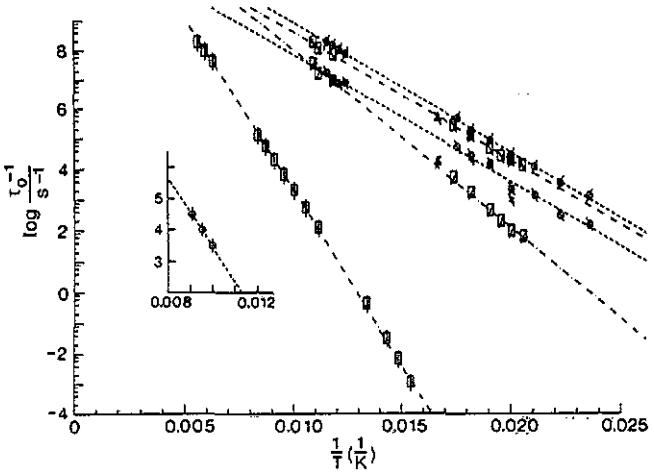

Figure 4. Logarithm of the inverse of the most probable relaxation time as obtained by fits to ε_{DW}, as a function of inverse temperature. Results for LF (|), HF1 (/) and HF2 (⊘) branches of the samples $K_{0.967}Li_{0.033}TaO_3$ (□) and $K_{0.974}Li_{0.025}TaO_3$ (○) are shown. Straight lines are the linear regressions defining the Arrhenius parameters in table 1. The chain curve corresponds to $K_{0.967}Li_{0.033}TaO_3$ and the broken curve to $K_{0.975}Li_{0.025}TaO_3$. Also shown are isolated data points for the samples $K_{0.966}Li_{0.034}TaO_3$ (△) and $K_{0.974}Li_{0.026}TaO_3$ (*), which allows the different growth methods to be compared. LF data points for $K_{0.975}Li_{0.025}TaO_3$ are shown in the inset because of overlap with $K_{0.967}Li_{0.033}TaO_3$ data.

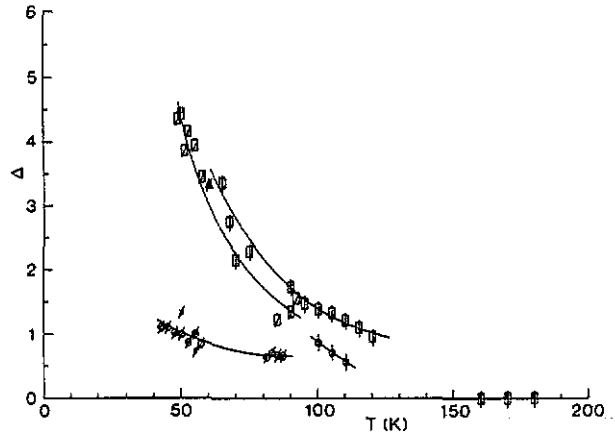

Figure 5. Width Δ of the Gaussian relaxation time distribution for the LF (|) and HF1 (/) branches for the samples $K_{0.967}Li_{0.033}TaO_3$ (□) and $K_{0.975}Li_{0.025}TaO_3$ (○). Also shown are isolated data points for the samples $K_{0.966}Li_{0.034}TaO_3$ (△) and $K_{0.974}Li_{0.026}TaO_3$ (*), which allows the comparison of different growth methods. Curves are guides to the eye.

(figure 4), and that both the relaxation step (figure 3) and the spread of the relaxation times (figure 5) increase monotonically with decreasing temperature.

Close inspection of the HF data shows that this dispersion curve exhibits a more complex structure than the LF branch. Fits to ε_{DW} (and to ε_{KKW} as described later), shown

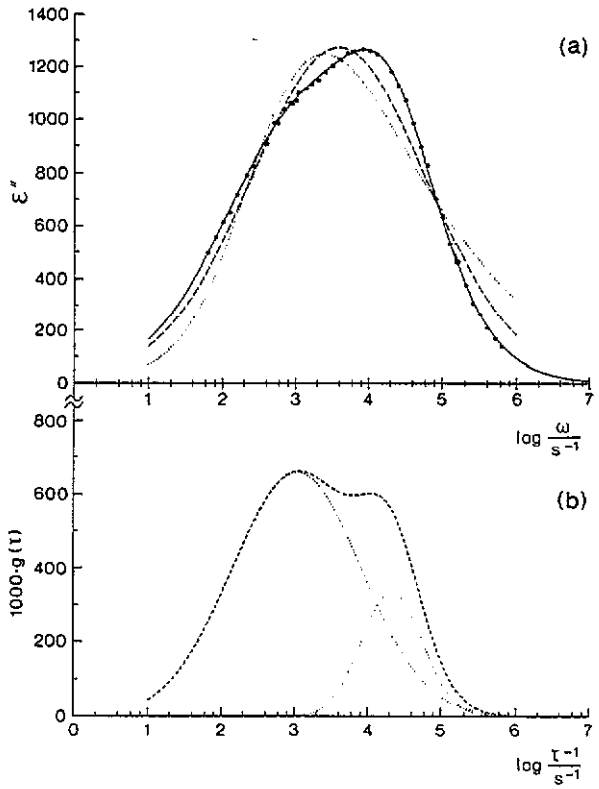

Figure 6. (*a*) Comparison of fits for the HF branch in the sample $K_{0.974}Li_{0.026}TaO_3$ at 50 K. The broken curve is the best fit of ε_{KWW} and the dotted curve is the fit of ε_{DW} to ε'' data. The full curve is the best fit of a distribution of logarithmic relaxation times given by a superposition of two Gaussian curves. (*b*) These two Gaussian curves are plotted against $\log(1/\tau)$ (dotted curves), together with the resulting distribution $g(log(1/\tau))$ (broken curve).

in figure 6 for the sample $K_{0.974}Li_{0.026}TaO_3$, are very unsatisfactory. In fact, these fits lead to variances that are much larger than the ones obtained from comparable data of the LF branch and the resulting parameters were devoid of any systematic temperature dependence. To improve the quality of the fits we used a superposition of two Gaussian curves, i.e. we suppose that the observed curve is the superposition of two different relaxation processes that we name HF1 and HF2, where HF1 is the dominant process. The resulting 6-parameter function fits the data with excellent accuracy and yields parameters with systematic temperature dependence. The corresponding distribution of relaxation times is also shown in figure 6 and it is seen that the separation of the two Gaussian curves is clearer in this representation than in the $\varepsilon''(\ln \omega)$ curves. We observe that this doubling is present in all samples, independent of growth method.

Figure 3 shows the relaxation strength for the two samples $K_{0.967}Li_{0.033}TaO_3$ and $K_{0.975}Li_{0.025}TaO_3$ and for the HF1 and LF branches as a function of temperature. In all cases, $\Delta\varepsilon$ grows more rapidly than T^{-1} when T is lowered: in fact, the expression $(T - T_0)^{-\gamma}$ can be fitted to the values of $\Delta\varepsilon$ with $\gamma > 2$ and $T_0 > 0$. The two relaxation branches have comparable strength in $K_{0.967}Li_{0.033}TaO_3$ whereas in $K_{0.975}Li_{0.025}TaO_3$ the high-frequency response is much stronger than the low-frequency one, which appears

Table 1.

Concentration x	LF	HF1	HF2
Energy barrier (E_b[K])			
2.5%	2550 ± 75	1000 ± 50	1000 ± 50
3.3%	2650 ± 75	1300 ± 50	1000 ± 50
Logarithm of attempt frequency ($\log_{10}[\nu_0$/Hz])			
2.5%	13.6 ± 0.5	12.1 ± 0.5	11.3 ± 0.5
3.3%	14.0 ± 0.5	13.1 ± 0.5	12.1 ± 0.5

to vanish for small Li concentrations (Höchli and Baeriswyl 1984). The fact that both branches are about equally strong in $K_{0.967}Li_{0.033}TaO_3$ allows their parameters to be evaluated with good and equal precision. For the control samples grown with a different method, they are practically identical.

The HF and LF branches are separated by several orders of magnitude in frequency at all temperatures: figure 4 shows $\ln(1/\tau_0)$ against T^{-1} for $K_{0.967}Li_{0.033}TaO_3$, $K_{0.975}Li_{0.025}TaO_3$ and, at some temperatures, for the control samples, again with identical results. Obviously the centre frequencies of the high-frequency branches decrease with increasing concentrations, whereas for the low-frequency branch the centre frequency is independent of x. For all branches, $1/\tau_0$ is nearly exponential in T^{-1}, such that Arrhenius parameters E_b/k_B and ν_0, defined by $\tau_0 = (2\pi\nu_0)^{-1}\exp(E_b/k_BT)$, can be determined. They are given in table 1. The width Δ of the distribution $g(\ln\tau)$ is shown in figure 5; it exhibits a strong increase with decreasing temperature.

5. Models of dielectric relaxation

The time-honoured Debye (1912) model implies that N dipoles p may occupy energetically equivalent sites, that they oscillate at a frequency ν_0 around one position and that once every period τ they hop to their neighbouring site. Here $\tau = (2\pi\nu_0)^{-1}\exp(E_b/k_BT)$, where E_b is the barrier between the two sites. The predictions of this model are exponential decay of the polarization and of the decay current $i(t)$. The susceptibility is given by $\Delta\varepsilon/(1 + j\omega\tau)$, where $\Delta\varepsilon = Np^2/3k_BT$. The two parameters $\Delta\varepsilon$ and τ are usually determined with least-square fits or from Cole–Cole plots (Coelho 1979). As a considerable amount of work has been done on the limiting behaviour of dielectric permittivities, we wish to mention that the Debye expression for very low and very high frequencies is characterized by its 'limits'

$$[a, b] = \left[\lim_{\omega\to 0}(\partial \ln \varepsilon''/\partial \ln \omega),\ \lim_{\omega\to\infty}(\partial \ln \varepsilon''/\partial \ln \omega)\right] = [1, -1]. \qquad (3)$$

Typical loss peaks in solids are broader than the Debye expression with a FWHM of 1.14 decades (Coehlo 1979). In order to fit the dielectric data, numerous generalized dielectric response or decay functions have been proposed, and most of them include the Debye expression as a special case. While some properties of different response functions have been studied previously (e.g. Lindsey and Patterson 1980) and limiting behaviour of the dielectric permittivity has been compared for the most frequently used functions (Hill and Jonscher 1983), the properties of the decay current have attracted

less attention. In the following overview of some expressions used to describe dielectric data, we thus wish to include the limiting behaviour of the decay current:

$$\{a, b\} \equiv \left\{\lim_{t\to 0} (\partial \ln i(t)/\partial \ln t), \lim_{t\to\infty} (\partial \ln t(t)/\partial \ln t)\right\}. \tag{4}$$

At the same time, we must stress that such limits can only be found experimentally through extrapolation, using data points at frequencies far from the centre of the loss peak. However, such data are often obtained with relatively poor precision. Moreover, different functions can lead to the same limiting behaviour, which is a clear indication that the shape of the loss curve around its centre frequency must be considered when testing different model predictions on experimental data.

In order to choose appropriate models, we will first focus on the two generalizations of the Debye expression for which a physical model related to our system has been proposed, namely a distribution of relaxation times and the Kohlrausch ('stretched exponential') decay, and then, for the sake of completeness, summarize properties of some other expressions.

The approach involving a distribution of relaxation times supposes that each relaxation time τ appears with a probability of $g(\tau)\,d\tau$. This implies that each process occurs at a different rate and independently of all others. It is then natural to relate $g(\tau)$ to a distribution of energy barriers. Symmetric distributions $g(E_b - E_{b0})$, centred at E_{b0}, of barriers in the Debye model give rise to log-symmetric distributions $g(\ln[\tau/\tau_0])$ and log-symmetric susceptibilities $\varepsilon''(\ln \omega\tau_0)$. In this distribution approach, the dielectric response function is calculated as a superposition of Debye relaxation phenomena. From a physics point of view, this only makes sense in the limit of weak interactions or for isolated dipoles. In all other cases, this parametrization in terms of a relaxation time distribution is simply a mathematical tool to extract some characteristics from the data, as was done in the previous section. Various distributions have been proposed, but only for the Gaussian argument $\ln(\tau/\tau_0)$ and width Δ (Wagner, 1913) are we aware of corresponding microscopic models. Most recently, Grannan *et al* (1990) obtained this distribution by Monte Carlo simulation for a model where elastic dipoles are randomly distributed in an elastic continuum. Neither the dielectric permittivity nor the decay current are known analytically. It can be shown, however, that the limiting behaviour of both the decay current and the permittivity are the same as that for a simple Debye process. Strictly speaking, since the minimum energy barrier is 0, any relation time distribution must be truncated such that $g(\tau) = 0$ for $\tau\nu_0 \leqslant 1$. This introduces some asymmetry in the case of a Gaussian distribution having a width Δ comparable to E_{b0}/k_BT. We believe that in the case $\Delta \ll E_{b0}/k_BT$, a Gaussian distribution seems to be a reasonable first assumption if random phenomena are considered. This does not hold for $\Delta > E_{b0}/k_BT$, i.e. where a truncation may lead to a significantly different result. We cannot, at this moment, imagine a physical model that would lead to a truncated distribution, although Macdonald (1987) has used it successfully to fit data from Birge *et al* (1984) for KBr:KCN.

Decay currents in conflict with exponential behaviour have often been expressed by the Kohlrausch (1847 and 1854) ('stretched exponential') function $F(t) = \Phi_0 \exp[-(\alpha t)^\beta]$. The corresponding $\varepsilon(\omega)$, calculated for the first time by Williams and Watts (1970) (for $\beta = 0.5$) and therefore called ε_{KWW}, is given for general values of β ($0 < \beta \leqslant 1$), by a series expansion (Williams *et al* 1971). It is found that

$$\left\{\lim_{t\to 0} (\partial \ln i/\partial \ln t), \lim_{t\to\infty} (\partial \ln i/\partial \ln t)\right\} = \{-\beta, -\infty\}$$

and that

$$\left[\lim_{\omega\to 0}(\partial \ln \varepsilon''/\partial \ln \omega), \lim_{\omega\to\infty}(\partial \ln \varepsilon''/\partial \ln \omega)\right] = [1, -\beta].$$

Several microscopic models have led to stretched exponential decay (Rajagopal *et al* 1984, Shlesinger and Montroll 1984, de la Fuente *et al* 1988) for certain classes of materials. The one that best applies to our system seems to be the approach of Palmer *et al* (1984). Here hierarchically constrained dynamics lead to series relaxation rather than parallel processes. Related models have been proposed following Palmer *et al*: Kumar and Shenoy (1986) show that hierarchical barriers as well as hierarchical constraints lead to this behaviour, and that these approaches are closely connected. Ultrametricity is introduced by energy barriers separating degenerate states in the Ogielski and Stein (1985) approach. In this system, the general exact solution for the dynamics is given and can lead to a KWW law with temperature-dependent β for one possible choice of these barriers. Finally it has been shown that the dynamics in ultrametric and hierarchical spaces are equivalent, even if the underlying coupling schemes are different (Knapp 1988).

Monte Carlo simulation of a simple Ising (± 1) spin glass with nearest-neighbour interactions leads to non-exponential decay that is best described by $f(t) = c(t/\tau)^{-x}\exp[-(t/\tau)^{\beta}]$, thus an additional parameter is introduced to generalize the KWW law (Ogielski 1985) (see also Binder 1990 for a short introduction to Monte Carlo simulation of glassy systems). The limiting behaviour of this decay current is characterized by $\{-x, -\infty\}$. It seems, however, that the KWW law describes well the data of simulation in more refined models, such as the three-state Potts glass (Wu 1982) if one takes the bonds J_{ij} in the Hamiltonian $\mathcal{H} = -\Sigma_{\langle i,j\rangle}J_{ij}\delta_{SiSj}$ to be a random variable with $P(J_{ij}) \propto \exp[-J_{ij}^2/2(\Delta J)^2]$ (Carmesin and Binder 1988), or such as the isotropic Edwards–Anderson model, where the Hamiltonian is given by $\mathcal{H} = -\Sigma_{\langle i,j\rangle}J_{ij}[(\Sigma_{\mu=1}S_i^{\mu}S_j^{\mu})^2 - \frac{1}{3}]$, again with Gaussian random bonds J_{ij} and where S_i is the μth component of a 3-component vector (Carmesin and Binder 1987).

We wish to conclude this section with the description of some other frequently used expressions. Obvious mathematical generalizations of the susceptibility are obtained by replacing the Debye expression $(1 = j\omega\tau)^{-1}$ by $(1 - [j\omega\tau]^m)^{-n}$, $0 < m, n < 1$. The generalization $n = 1$, m variable, is by Cole and Cole (1941) and gives rise to a susceptibility $\varepsilon''(\ln \omega\tau)$ which is symmetric in the argument and has the limits $[+m, -m]$. The opposite case, $m = 1$, n variable, proposed by Davidson and Cole (1951) yields limits $[1, -n]$. The double generalization is by Havriliak and Negami (1966). With $[m, -m \times n]$ as its limits, it quite generally fits the data, which is to be expected in view of the larger number of parameters. It is worth noting that the Fourier transform of the 4-parameter Havriliak–Negami function can be fitted to the 3-parameter stretched exponential decay with good precision provided that the parameters m and n are related (Macdonald and Hurt 1986). To our knowledge, analytical expressions of the decay current for the case $m \neq 1$ exist for only $m = 1/2$ in terms of parabolic cylinder and error functions. For the Cole–Davidson expression, however, the inverse Laplace transform is evaluated analytically (Roberts and Kaufman 1966) to yield $i(t) = \Delta\varepsilon\,\varepsilon_0 E_0(\tau^n\Gamma(n))^{-1}t^{n-1}\exp[-t/\tau]$, with limits $\{n - 1, -\infty\}$. Note that this function can be seen as a special case of the Ogielski (1985) expression, with $x = n - 1$ and $\beta = 1$. These mathematical generalizations of the Debye expressions are not based on microscopic models.

Another approach leading to non-exponential relaxation has to be mentioned in this

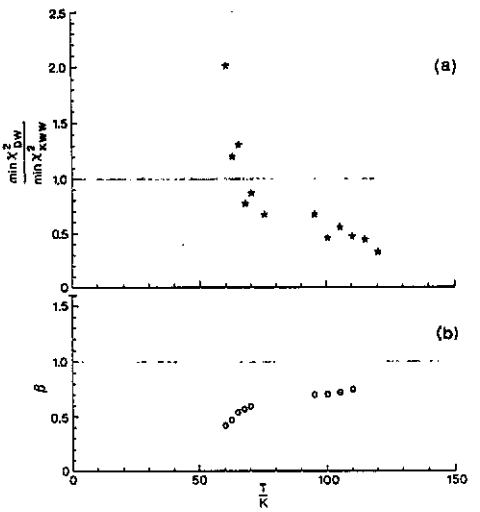

Figure 7. (*a*) Comparison of the variances of fits to data for the $K_{0.967}Li_{0.033}TaO_3$ sample. Points above the dotted horizontal line indicate that the data are represented better by the KWW function than by the one resulting from a log–Gaussian distribution of relaxation times. (*b*) KWW fit parameter β for the same sample. β increases monotonically with T. Such behaviour has been proposed independently by Carmesin and Binder (1988) and by Palmer *et al* (1984).

context. In their cluster model, Dissado and Hill (1987) find an equation of motion

$$d^2\Phi(t)/dt^2 + t^{-1}(2 + n + \omega_p t)d\Phi(t)/dt + t^{-2}[n + \omega_p t(1 + m)]\Phi(t) = 0$$

which has an analytical solution in terms of a Gaussian hypergeometric function for both the decay and the dielectric response. Their limits are $\{-n, -(1 + m)\}$ and $[m, n - 1]$, which account well for behaviour of a large number of materials. The resulting function has one more parameter than the KWW law and it should therefore be expected to fit many data sets better. At the same time we must note that this model does not seem to allow for temperature dependence of the parameters n and m. This implies that the shape of the loss curve does not change with temperature, and in particular that its width is constant, contrary to what we observe in $K_{1-x}Li_xTaO_3$.

6. Interpretation

If we select expressions with a microscopic background, the choice is reduced to the Kohlrausch (stretched exponential decay function) and the Debye–Wagner (log-Gaussian superposition of relaxation times) expressions. We fitted both functions to the complete data sets over all temperatures attained in the experiment and calculated the corresponding minimum χ^2 values for each function as a measure of the quality of the fit. For most of the dispersions studied here, the Debye–Wagner function leads to a smaller minimum χ^2 than the Kohlrausch expression does, indicating that the Debye–Wagner function describes the data better. However, for the one relaxation phenomenon that can be observed over most of the 12-decade interval, namely the LF dispersion in the $K_{0.967}Li_{0.033}TaO_3$ sample, a crossover from Debye–Wagner to Kohlrausch behaviour is observed as T decreases (figure 7). For this sample, the ratio of the minimum χ^2 values rises steadily from 0.3 to 2 as the temperature is lowered from 120 to 50 K, indicating a crossover from independent dipole behaviour to hierarchical relaxation around $T = 65$ K. In the temperature interval where the Kohlrausch expression fits the data better than or as well as a Gaussian distribution of relaxation times ($T \leqslant 70$ K), the β parameter decreases with decreasing temperature (figure 7*b*). This is in agreement

with Monte Carlo simulations of the Edwards–Anderson model for quadrupolar glasses (Carmesin and Binder 1987).

Turning now to the nature of dipole motion associated with each relaxation branch, we first consider the high-frequency relaxation, i.e. flips by $\pi/2$. Dielectric data published by Van der Klink *et al* (1983) for Li concentrations from 1% to 6% show that the motion becomes progressively slower as the concentration increases but the energy barrier remains close to 1100 K (±200 K) for all concentrations.

Considering that the barrier corresponding to these $\pi/2$ flips is about half that for π flips, and taking the probability for a Li ion to jump over a barrier to be $\tau^{-1} = (2\pi\nu_0)\exp[-E_b/k_BT]$, we see that this probability is orders of magnitude larger for $E_b = 1100$ K than for $E_b = 2500$ K. Thus we should find that the larger barrier has virtually no influence on the relaxation time of the system. This holds if both paths for fluctuations of moments, by $\pi/2$ and by π flips, are open, and is observed in the low-concentration limit. In fact, the only relaxation branch observed in these low-concentration samples ($x \leqslant 2\%$) corresponds to $E_b \sim 1100$ K (Höchli and Maglione 1989).

In some case (figure 6), neither a simple Debye–Wagner nor a Kohlrausch function describes the HF-branch data satisfactorily. We relate this observation to a model calculation by Van Weperen *et al* (1977), who found that the probability distribution of dipole–dipole interaction energies for randomly displaced Ce^{3+} ions in SrF_2 was not Gaussian but had more than one local maximum. Sheng and Chen (1988) studied the local-field distribution in random dielectric media as a function of dipole concentration and polarizability by generalizing Onsager's reaction field approach. Their results indicate that the local-field distribution is generally double-peaked. Also, the separation between the two peaks varies linearly as a function of the particle polarizability, which explains why this double-peak characteristic is not always observed: clearly, the two peaks merge at low polarizabilities. The splitting of the field distribution into two local maxima is a consequence of nearest-neighbour interaction (Chen and Sheng 1991). This is similar to what one concludes from a generalized random local field theory, which considers pair interaction in more detail and where two maxima can also be observed (Vugmeister and Stephanovich 1988, Vugmeister and Glinchuk 1990).

In the present paper, we describe this double-peak characteristic quantitatively by fitting a double-Gaussian distribution of relaxation times to the susceptibility data. We observe that the relaxation step corresponding to the first Gaussian curve (HF1) is much larger than the one for the second (HF2). Therefore, we can limit ourselves to the discussion of the HF1 peak, and deduce a detailed description of the $\pi/2$ impurity motion from the temperature dependence of characteristic parameters of this peak.

First consider that the interaction between multipoles grows as the concentration increases and as the temperature decreases: this interaction leads to the observed spread Δ of the relaxation times with increasing concentration and decreasing temperature. In the context of Chen and Sheng's study (1991), this can be interpreted as a consequence of growing anisotropy, i.e. of local ordering and the formation of coherently moving clusters, which have also been observed by Azzini *et al* (1991). At the same time, the relaxation step grows faster than $1/T$ with decreasing temperature, another indication that the multipole movements are correlated, and is larger in higher-concentration samples as long as $x \leqslant 0.04$. However, as the critical concentration ($x \sim 0.04$) is approached, the multipolar interaction becomes a hindering factor on impurity motion. This is clearly observed in our $x = 0.033$ sample: still considering the HF1 relaxation branch only (Symbol ⊠ in figure 3), we see that the relaxation step goes through a maximum at $T \simeq 52$ K, while the spread Δ of the relaxation times exhibits no special

feature at this temperature. This temperature is sometimes called the freezing temperature (T_f)—a practical but potentially misleading term since motion does not come to a half at 52 K, nor does its slowing down deviate from the Arrhenius curves (figure 4).

How can this particular behaviour at T_f—a maximum of $\Delta\varepsilon$ but no critical slowing down—be understood? We suggest that the correlated motion of the impurities takes place by changing the polarization of a group of impurities, or a cluster, simultaneously. For randomly distributed multipoles, the total interaction energy between all dipoles belonging to the same cluster will change, in general, if all moments flip by $\pi/2$. This causes these movements to be less likely if interactions are important. One expects interaction to be important if the lattice polarization arising from one impurity is important at the site of its neighbour. A recent theoretical study based on a nonlinear shell model (Stachiotti *et al* 1991) shows that this polarization extends over $d \simeq 3a$, where a is the lattice constant, and therefore becomes important if the average available volume per impurity, $1/x$, becomes comparable to d^3, i.e. if $x \simeq 4\%$, as found in the experiment. Thus for some of the local configurations found in the random distribution of impurities, this interaction inhibits flips by $\pi/2$, leading to the decrease of the relaxation step, while motion of other configurations continues to slow down according to an Arrhenius law.

Flips by π are not subject to the same hindering interaction: the quadrupolar moment does not change in this motion, nor does the internal energy of a cluster of coherently moving dipoles. Therefore jumps over the 2500 K barriers, which would be very rare if the much faster $\pi/2$ flips ($E_b \simeq 1100$ K) were allowed, will be observed for those clusters for which $\pi/2$ motion is hindered, i.e. when interactions between multipoles play an important role. This is observed in $K_{0.967}Li_{0.033}TaO_3$, where the relaxation strength of the π branch (symbol ⊡ in figure 4) becomes stronger than the one corresponding to $\pi/2$ motion (symbol ⊠) below a certain temperature. While interaction between dipoles belonging to the same cluster does not change if the polarization of the configuration is inverted and does not hinder this π motion, interactions with neighbouring clusters will. This allows us to model a whole cluster as one multipole, as is sometimes done in spin glasses (Binder and Young 1986). Interaction between these (cluster) multipoles leads to the observed distribution of relaxation times at intermediate temperatures, whereas for higher temperatures (and therefore for smaller interactions) the motion is quite close to being monodispersive. At even lower temperatures, however, the motion crosses over from Debye–Wagner to Kohlrausch-type behaviour. We postulate that flips by π are only possible, at low temperatures, if the surrounding configuration is favourable, thus leading to hierarchically constrained motion. This corresponds exactly to the model by Palmer *et al* (1984), where cluster A cannot move until cluster B moves out of the way, and therefore a hierarchy of degrees of freedom from fast to slow is established. In this model, the levels $n = 0$ (fastest), 1, 2, . . . are represented by N_n pseudospins, and level $n + 1$ can change only if μ_n pseudospins at level n attain one particular state. By postulating $\mu_n = \mu_0 n^{-p}$ with $p = 1 + \varepsilon$, and $N_{n+1} = N_n/\lambda$, $\lambda < 1$, one obtains Kohlrausch-type behaviour for $\varepsilon \ll 1$ and a stretching variable given by $\beta = (1 + \mu_0 \ln 2)^{-1}$. This relates β^{-1} linearly to the number of pseudospins at level n that need to be in one particular state in order to allow the pseudospins at level $n + 1$ to flip, and this number is expected to grow as temperature decreases. The consequence that β is an increasing function of the temperature is well observed experimentally (figure 7(*b*)).

7. Conclusion

Two relaxation branches are revealed in $K_{1-x}Li_xTaO_3$: one based on $\pi/2$ motion, the other on π motion of the dipoles. The $\pi/2$ (HF) branch is dominant at low concentration

and the π (LF) branch dominates at high Li concentrations. At an intermediate concentration of 3.3% both branches are present and their characteristics allow us to deduce that:

(i) The $\pi/2$ (HF) motion is related to barriers of ~1000 K. The interaction of displaced Li impurities with the lattice and other impurities grows with increasing concentration and decreasing temperature. This leads to a spread of the energy barriers, and to the formation of coherently moving clusters. For relatively weak interaction, the relaxation step grows with growing interaction, but when interactions between multipoles belonging to the same cluster become more important, they hinder this motion and lead to a decrease of the HF-branch relaxation step at high concentrations and low temperatures.

(ii) Impurities for which $\pi/2$ flips are restrained by intra-cluster interactions are still free to flip by π, even if the corresponding energy barrier is much larger (~2500 K), giving rise to the LF relaxation branch. The observed spread of the energy barriers and the increase of the relaxation step is mainly due to interaction between different clusters. This cluster–cluster interaction is such that π flips of clusters do not remain independent at low temperatures. Here, a hierarchy of levels (from fast to slow) is established, as evidenced by Kohlrausch-type relaxation below a crossover temperature of ~65 K.

References

Azzini G A, Banfi G P, Giulotto E and Höchli U T 1991 *Phys. Rev.* B **43** 7473

Bellman R, Kalaba R E and Lockett J A 1966 *Numerical Inversion of the Laplace Transform* (New York: Elsevier)

Binder K 1990 *Ferroelectrics* **104** 3

Binder K and Young A P 1986 *Rev. Mod. Phys.* **58** 801

Birge N O, Jeong Y H, Nagel S R, Bhattacharya S and Susman S 1984 *Phys. Rev.* B **30** 2306

Carmesin H-O and Binder K 1987 *Europhys. Lett.* **4** 269

Carmesin H-O and Binder K 1988 *J. Phys. A: Math. Gen.* **21** 4053

Chen Z and Sheng P 1991 *Phys. Rev.* B **43** 5735

Coelho R 1979 *Physics of Dielectrics for the Engineer* (Amsterdam: Elsevier)

Cole K S and Cole R H 1941 *J. Chem. Phys.* **9** 341

Colonomos P and Gordon R G 1979 *J. Chem. Phys.* **71** 1159

Davidson D W and Cole R H 1951 *J. Chem. Phys.* **19** 1417

de la Fuente M R, Pérez Jubindo M A and Tello M J 1988 *Phys. Rev.* B **37** 2094

Debye P 1912 *Z. Phys.* **13** 97

Dissado L A and Hill R M 1987 *Solid State Ionics* **22** 331

Doussineau P, Frènois C, Levelu A, Zielkiewicz S and Höchli U T 1991 *J. Phys.: Condens. Matter* **3** 8369–75

Elwell D and Scheel H J 1975 *Crystal Growth from High Temperature Solutions* (London: Academic) pp 386–95

Grannan E R, Randeria M and Sethna J P 1990 *Phys. Rev.* B **41** 7784

Havriliak D W and Negami S 1966 *J. Polymer Sci.* C**14** 99

Hill R M and Jonscher A K 1983 *Contemp. Phys.* **24** 75

Höchli U T 1982 *Phys. Rev. Lett.* **48** 1494

Höchli U T and Baeriswyl D 1984 *J. Phys. C: Solid State Phys.* **17** 311

Höchli U T, Hessinger J and Knorr K 1991 *J. Phys.: Condens. Matter* **3** 8377–85

Höchli U T, Knorr K and Loidl A 1990 *Adv. Phys.* **39** 405

Höchli U T and Maglione M 1989 *J. Phys.: Condens. Matter* **1** 2241

Jonscher A K 1983 *Dielectric Relaxation in Solids* (London: Chelsea Dielectric)

Knapp E W 1988 *Phys. Rev.* B **38** 2664

Kohlrausch R 1847 *Ann. Phys., Lpz.* **12** 393

Kohlrausch R 1854 *Poggendorff Annalen der Physik* **91** 179

Kumar D and Shenoy S R 1986 *Solid State Commun.* **57** 927

Lindsey C P and Patterson G D 1980 *J. Chem. Phys.* **73** 3348

Macdonald J R 1987 *J. Appl. Phys.* **61** 700
Macdonald J R and Hurt L 1986 *J. Chem. Phys.* **84** 496
Maglione M 1987 *PhD Thesis* No 667 EPF Lausanne Switzerland
Ogielski A T 1985 *Phys. Rev. B* **32** 3784
Ogielski A T and Stein D L 1985 *Phys. Rev. Lett.* **55** 1634
Palmer R G, Stein D L, Abrahams E and Anderson P W 1984 *Phys. Rev. Lett.* **53** 958
Prater R L, Chase L L and Boatner L A 1981 *Phys. Rev.* B **23** 5904
Press W H, Flannery B P, Teukolsky S A and Vetterling W T 1986 *Numerical Recipes: The Art of Scientific Computing* (Cambridge: Cambridge University Press) p 523
Rajagopal A K, Teitler S and Ngai K L 1984 *J. Phys. C: Solid State Phys.* **17** 6611
Roberts G E and Kaufman H 1966 *Table of Laplace Transforms* (Philadelphia and London: W B Saunders) p 207
Sheng P and Chen Z 1988 *PHys. Rev. Lett.* **60** 227
Shlesinger M F and Montroll E W 1984 *Proc. Natl Acad. Sci. USA* **81** 1280
Stachiotti M G, Migoni R L and Höchli U T 1991 *J. Phys.: Condens. Matter* **3** 3689
van der Klink J J and Rytz D 1982 *J. Cryst. Growth* **56** 673
van der Klink J J, Rytz D, Borsa F and Höchli U T 1983 *Phys. Rev.* B **27** 89
van Weperen W, Lenting B P M, Bijvank E J and den Hartog H W 1977 *Phys. Rev.* B **16** 2953
Vugmeister B E and Glinchuck M D 1990 *Rev. Mod. Phys.* **62** 993
Vugmeister B E and Stephanovich V A 1988 *Solid State Commun.* **66** 673
Wagner K W 1913 *Ann. Phys., Lpz.* **40** 817
Williams G and Watts D C 1970 *Trans. Faraday Soc.* **66** 80
Williams G, Watts D C, Dev S B and North A M 1971 *Trans. Faraday Soc.* **67** 1323
Wu F Y 1982 *Rev. Mod. Phys.* **54** 235